

SOLAR THERMAL PROCESS PARAMETERS FORECASTING FOR EVACUATED TUBE COLLECTORS (ETC) BASED ON RNN-LSTM

MUHAMMAD ALI AKBAR¹, AHMAD JAZLAN¹, MUHAMMAD MAHBUBUR
RASHID^{1*}, HASAN FIRDAUS MOHD ZAKI¹, MUHAMMAD NAVEED AKHTER²
AND ABD HALIM EMBONG¹

¹*Department of Mechatronics Engineering, Kulliyah of Engineering,
International Islamic University Malaysia, Kuala Lumpur, Malaysia.*

²*Department of Electrical Engineering,
Rachna College of Engineering and Technology Gujranwala 52250
(A Constituent college of University of Engineering and Technology Lahore), Pakistan*

*Corresponding author: mahbub@iium.edu.my

(Received: 28th March 2022; Accepted: 22nd August 2022; Published on-line: 4th January 2023)

ABSTRACT: Solar Heat for Industrial Process (SHIP) systems are a clean source of alternative and renewable energy for industrial processes. A typical SHIP system consists of a solar panel connected with a thermal storage system along with necessary piping. Predictive maintenance and condition monitoring of these SHIP systems are essential to prevent system downtime and ensure a steady supply of heated water for a particular industrial process. This paper proposes the use of recurrent neural network-based predictive models to forecast solar thermal process parameters. Data of five process parameters namely - Solar Irradiance, Solar Collector Inlet & Outlet Temperature, and Flux Calorimeter Readings at two points were collected throughout a four-month period. Two variants of RNN, including LSTM and Gated Recurrent Units, were explored and the performance for this forecasting task was compared. The results show that Root Mean Square Errors (RMSE) between the actual and predicted values were 0.4346 (Solar Irradiance), 61.51 (Heat Meter 1), 23.85 (Heat Meter 2), Inlet Temperature (0.432) and Outlet Temperature (0.805) respectively. These results open up possibilities for employing a deep learning based forecasting method in the application of SHIP systems.

ABSTRAK: Penggunaan sumber bersih seperti Tenaga Solar dalam Proses Industri (SHIP) adalah satu kaedah alternatif untuk menghasilkan tenaga yang boleh diperbaharui bagi mengurangkan kesan gas rumah hijau yang terhasil dari proses industri. Sistem SHIP biasanya mengandungi panel solar dan sistem penyimpanan haba yang berhubung melalui paip yang sesuai. Penyelenggaraan secara berkala diperlukan bagi memastikan sistem ini sentiasa membekalkan tenaga solar pada kadar bersesuaian dan bekalan tenaga solar yang terhasil berterusan dan tidak menjejaskan sistem pemanasan air bagi sesuatu proses industri. Kajian ini mencadangkan penggunaan model ramalan rangkaian neural berulang bagi meramal parameter proses pemanasan solar. Kelima-lima parameter proses iaitu – Iradiasi Solar, Suhu Saluran Keluar & Masuk Pengumpul Solar dan Bacaan Kalorimeter Fluks pada dua tempat diambil sepanjang empat bulan (dari Julai 2021 sehingga Oktober 2021). Dapatan menunjukkan dua varian RNN termasuk LSTM dan Unit Berulang dapat dibanding prestasinya bagi tugas ramalan ini. Dapatan kajian menunjukkan Ralat Punca Min Kuasa Dua (RMSE) antara bacaan sebenar dan ramalan adalah masing-masing 0.4346 (Iradiasi Solar), 61.51 (Meter Terma 1), 23.85 (Meter

Terma 2), Suhu Salur Masuk (0.432) and Suhu Salur Keluar (0.805). Ini membuka peluang kajian mendalam berdasarkan kaedah ramalan dalam aplikasi sistem SHIP.

KEYWORDS: *evacuated tube collectors; solar irradiance; flux calorimeter; recurrent neural networks; long short term memory*

1. INTRODUCTION

More than 80% of energy generation in today's world is sourced from non-renewable energy resources such as coal, natural gas, and oil [1-3]. The reduction of fossil fuel resources worldwide combined with increased environmental concerns have resulted in a higher demand for renewable and cleaner energy such as solar, wind, hydroelectric, biofuels, piezoelectric and RF energy. Oleochemical industries commonly utilize Natural Gas (NG) for generating low, medium, and high temperature heating, which is required as part of the overall Oleochemical process flow. However, NG-based heating is known to increase undesirable Greenhouse Gas emissions [4].

In Malaysia, solar energy is viewed as a viable, sustainable energy source due to the sunlight availability throughout the year, which is attributed to the tropical climate. Therefore, historically, solar energy has been widely utilized for both residential and commercial water heating applications. Evacuated Tube Collectors (ETC) and Flat Plate Collectors (NC-FPC) are the two most commonly used solar collectors for low to medium temperature industrial and residential water heating applications. These solar collectors are connected to thermal storage systems to allow energy to accumulate. Therefore, when solar irradiation is at its highest during the day, it enables energy to continue to be delivered. On the other hand, solar irradiation is at its lowest or utterly unavailable during rainy weather or at night, therefore, no energy can be delivered. Thermal storage systems consist of various heating equipment such as pumps, heat exchangers, electrical boilers, and gas boilers. A typical complete Solar Heat for Industrial Process (SHIP) system, at its simplest, consists of a control system, water circulation pump with power supply, hot & cold water storage tanks, piping, monitoring systems and a heat exchanger.

To ensure the long-term performance of the overall system and minimize downtime, condition monitoring as well as predictive maintenance of this heating equipment are essential. The ability to forecast, identify, and locate when and where a fault may occur in one part of this equipment and its sub-processes will save maintenance costs and prevent long-term damages to the overall system. Machine learning based models describing an industrial process are useful for applications such as anomaly detection, fault diagnosis and forecasting future system characteristics. The Remaining Useful Life (RUL) of equipment such as pumps, valves, compressors and batteries refers to the time interval before the equipment experiences failure [5-7]. Knowledge about the RUL of an equipment is crucial for maintenance engineering practices and engineering system reliability analysis in a plant. RUL can be forecast using suitable machine learning models. Previous studies have demonstrated the applicability of machine learning models for the analysis of rotating mechanical equipment using sound and vibration measurements, encoder data and temperature measurements [8]. Machine learning models are highly data-driven and therefore require high-quality data of a particular process to generate meaningful results. Effective measurement and data preprocessing methods are essential.

Recurrent Neural Networks (RNN) are a category of Artificial Neural Networks (ANN) that work well with time-series data in various applications such as speech recognition and language translation. RNN are the basis for widely used tools worldwide,

namely Google Translate and Siri by Apple [9]. Similarly to convolutional and feedforward neural networks, RNN also use training data for learning. The difference is that RNN utilize information from prior inputs to affect current inputs and outputs. Traditional convolutional and feedforward neural networks also have a disadvantage since inputs and outputs are assumed to be independent of each other. Long Short Term Memory (LSTM) RNN is a modified version of the standard RNN with promising performance. LSTM RNN has successfully been applied in biomedical signal classification, radar target classification, keyword detection, text generation, and video classification [10-15].

This paper presents the design and development of an Evacuated Tube Solar Heat for Industrial Process (SHIP) system to generate the thermal energy required in an oleochemical plant. This plant manufactures fatty acids, glycerin, and soap noodles that are the base material for many types of industrial processes such as the manufacturing of household and toilet detergents. A Long Short-Term Memory Recurrent Neural Network (LSTM-RNN) was used to forecast Solar Irradiance, Solar Collector Inlet/Outlet Temperature, and Flux Calorimeter readings collected throughout a four (4) month period starting from July 2021 and ending in October 2021. Existing studies on forecasting of such parameters were carried out only on smaller-scale experimental prototypes. In contrast, in this study, forecasting was carried out for the first time on a larger scale industrial-grade Evacuated Tube Collector solar thermal system installed in Malaysia. Forecasting of these parameters is essential for the estimation of throughput and of future Return of Investments (ROI).

2. PRELIMINARIES

2.1 Overview of Installed SHIP System and Data Collection

Experimental work and data collection were carried out at an Oleochemical Process Plant based in Malaysia. The Solar Heat for Industrial Process (SHIP) at this factory was implemented using a total of 75 Evacuated Tube Collector Solar Panels (Linuo Ritter - Model CPC 1518). Each of these 75 solar panels consisted of 18 evacuated tubes. In this factory, solar energy heating was utilized as an energy-efficient replacement for existing legacy gas boilers. Evacuated Tube Solar Collectors have a useful life ranging between 20-25 years. Therefore, they are a viable option for achieving a long-term Return of Investment (ROI) [16-18]. This SHIP system was installed at $01^{\circ}28'57''$ latitude and $103^{\circ}54'25''$ longitude coordinates. This location was selected to avoid the impact of shading effects which would cause a significant reduction of the solar panel efficiency [19-23]. Reviews on various factors affecting solar energy performance and machine learning methods applied in the context of solar energy have been described in previous studies [24-26].

The solar panels were positioned on the roof directly above the boiler at an inclined angle of 10° , as shown in Fig. 1 and Fig. 2. This 10° inclined angle selection was based on the manufacturer's recommendation to maximize the solar energy that can be generated from the solar panels. The cumulative surface area of these 75 solar panels was 225 m^2 . The total elevation of the solar panels relative to sea level was 16.35 meters. Solar Irradiance was measured using a Solar Pyranometer Radiation Sensor (RIKA - RK 200-03) which was installed at the roof top close to the ETC. Five process parameters namely Solar Irradiance, Solar Collector Inlet/Outlet Temperatures, and Flux Calorimeter readings from two points were recorded throughout a 4-month period starting from July 2021 until October 2021.

Solar Irradiance and Solar Collector Inlet and Outlet temperature were collected daily starting from 8:00 AM until 7:00 PM with a sampling rate of 15 minutes. Flux Calorimeter readings were collected hourly every day from 8:00 AM until 7:00 PM. The data collected for each process parameter can be represented as a single time series with time steps corresponding to either 15 minutes or 1 hour accordingly. This data was then used in an LSTM network for the prediction of future process data.



Fig. 1: Array of Evacuated Tube Collectors (front view).



Fig. 2: Array of Evacuated Tube Collectors (side view with 10 degree inclination).

2.2 Process Flow and its Description

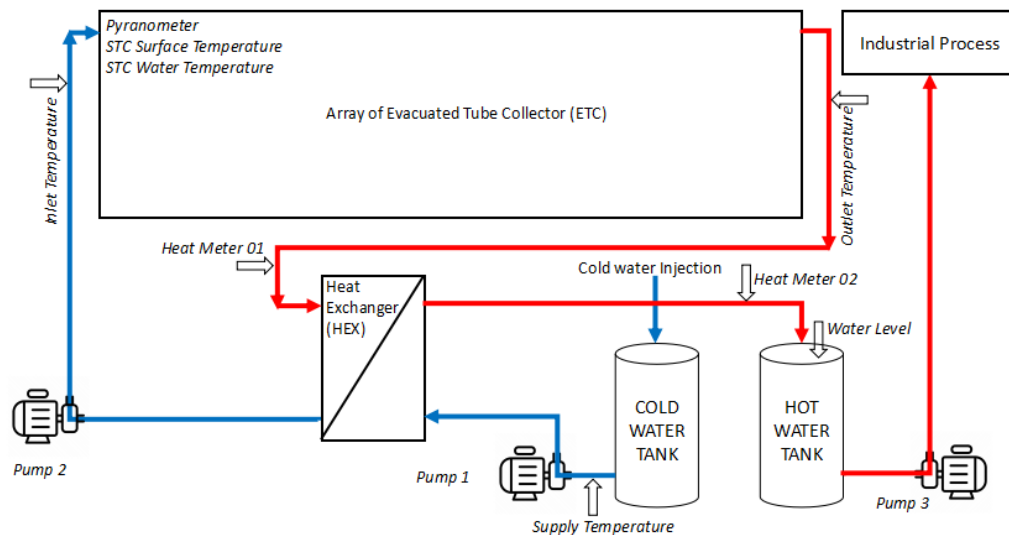


Fig. 3: Overall Process Flow Diagram for SHIP System.

The overall process flow diagram of the Evacuated Tube Solar Heat for Industrial Process (SHIP) System which was implemented at a Malaysian Oleochemical Process Factory is shown in Fig. 3. The blue arrows indicate the flow pipes, whereas the red arrows indicate the return pipes with heated water. The process starts by supplying cold water to the cold-water tank, which can store a maximum volume of 20 m³ of water (cold water injection). A pump (pump 1) will then control the flow of water from the outlet of the cold storage tank to the inlet of the heat exchanger. The flow rate of the water being transferred from the cold storage tank to the heat exchanger is fixed at 5.5 m³/hour. A second pump (pump 2) will control the flow of water circulation from the first outlet of the heat exchanger to the array of Evacuated Tube Collectors, generating hot water, which will be delivered to the hot water tank through the heat exchanger.

A flux calorimeter (Heat Meter 1) is used to monitor the thermal energy of the hot water circulating from the array of Evacuated Tube Collectors back into the heat

exchanger. This flux calorimeter is equipped with a flow meter and two temperature sensors at both the flow and return pipes. The flux calorimeter device calculates the temperature difference between the flow and return pipes. This temperature difference is multiplied by the volume of the water measured by the flow meter and the hot water's thermal coefficient resulting in the final readings in Kilo-Watt Hour (kWh). The flow rate of the water circulating from the first output of the heat exchanger to the array of Evacuated Tube Collectors and back to the heat exchanger is fixed at 5.5 m³/hour. The hot water from the heat exchanger is then allowed to flow into a Hot Water Storage Tank, which can store a maximum volume of 20 m³ of water.

Industrial grade ultrasonic long body sensors are placed at the top of the Hot Water storage tanks for liquid level monitoring. These industrial-grade ultrasonic sensors can work in harsh environments and are unaffected by moisture, debris, or heat. A second flux calorimeter (Heat Meter 2) is used to monitor the thermal energy of the hot water which is circulating from the heat exchanger into the Hot Water Storage Tank. Finally, a third pump (pump 3) will be used to deliver the water from the Hot Water Storage Tank to the oleochemical industrial process. In this process, the input parameters are the Solar Irradiance and ETC inlet temperature. The intermediate parameters are the readings from Heat Meter 1 & 2. The output parameter is the ETC outlet temperature. In this paper, all these 5 parameters will be forecast using an LSTM Regression network.

The data presented in Table 1 shows that the value of Solar Irradiance continuously fluctuates between 50 W/m² and 95 W/m². This fluctuation is expected since Solar Irradiance commonly peaks during midday before gradually declining in the evening. Furthermore, the Collector Inlet Temperature fluctuates between 26 and 65 degrees Celsius, as reflected in Table 2. The first flux calorimeter (Heat Meter 1) readings have a higher fluctuation range (between 0 kWh and 360 kWh). Whereas the second flux calorimeter (Heat Meter 2) readings vary between 0-125 kWh, as reflected in Tables 1 and 2. Finally, the solar collector outlet temperature which represents the temperature of the water heated by the solar irradiation fluctuates between 25 and 70 degrees Celsius, as reflected in Table 3. This heated water will then be delivered for use at a particular oleochemical processing stage.

Table 1: minimum, maximum, and mean values for solar irradiance and flux calorimeter (Heat Meter 1) readings

Month	Solar Irradiance (W/m ²)			Heat Meter 1 (kWh)		
	Min	Max	Mean	Min	Max	Mean
July	54.80	83.70	68.20	2.60	302.80	139.30
August	50.80	86.70	70.10	0.04	283.00	150.40
September	54.80	93.70	72.50	0.03	300.10	144.50
October	53.80	94.60	74.50	0.57	366.70	171.60

Table 2: Minimum, maximum, and mean values for flux calorimeter (Heat Meter 2) and solar inlet temperature readings

Month	Heat Meter 2 (kWh)			Solar Inlet Temperature (Celsius)		
	Min	Max	Mean	Min	Max	Mean
July	0.10	98.60	43.80	26.00	65.70	38.00
August	0.05	114.20	38.50	26.00	55.00	37.00
September	0.03	116.40	47.80	27.00	48.00	34.40
October	0.06	124.90	45.20	27.00	48.00	35.00

Table 3: Minimum, maximum, and mean values for solar inlet temperature readings

Month	Solar Outlet Temperature (Celsius)		
	Min	Max	Mean
July	24.90	70.00	40.30
August	26.00	68.70	39.00
September	25.80	63.50	37.80
October	26.80	65.70	38.40

3. METHODOLOGY

3.1 LSTM-RNN based Forecasting

This section describes the forecasting of time series data collected from the Solar Heat for Industrial Process (SHIP) system by using Long Short-Term Memory Networks (LSTM). Future time steps of a time series sequence can be forecast by training a sequence-to-sequence LSTM network such that the outputs to the network are the input sequence shifted ahead by one time step. At a particular time step of the input sequence, the LSTM network learns to forecast the values at the following time step. The time series data of Solar Irradiance, Flux Calorimeters (Heat meters 1 & 2), Solar Collector Inlet & Outlet Temperature were each partitioned into training and test data. In each case the first 90% of the time series data sequence was used as the training data and the remaining 10% of the time series data sequence was used as the testing data. Standardization/Normalization of the training data was performed in order to achieve a better fit and convergence of the LSTM RNN training. Firstly, the mean of the training data is calculated using Eq.(1) as follows:

$$\mu = \frac{\sum X}{N} \quad (1)$$

Where μ is the mean of the training data, $\sum X$ is the summation of all the elements in the training data and N is the total number of elements in the training data. Secondly, the standard deviation of the training data is calculated using Eq.(2) as follows:

$$\sigma = \sqrt{\frac{\sum (X_i - \mu)^2}{N}} \quad (2)$$

Where σ is the standard deviation of the training data and X_i is each element in the training data. The normalization of the training data, \bar{X}_i can then be found using Eq.(3) as follows:

$$\bar{X}_i = \frac{X_i - \mu}{\sigma} \quad (3)$$

Forecasting the values of future time steps in a sequence of data is then done as follows. Two vectors that consist of data extracted from the training data are defined as:

$$\text{Predictors} = [\bar{X}_i, \bar{X}_{i+1}, \bar{X}_{i+2}, \bar{X}_{i+3}, \dots, \bar{X}_{N-1}]$$

$$\text{Responses} = [\bar{X}_{i+1}, \bar{X}_{i+2}, \bar{X}_{i+3}, \bar{X}_{i+4}, \dots, \bar{X}_N]$$

The responses are simply the values of the training data shifted by one time step. The predictors are the training data, excluding the final time step. At a particular time step \bar{X}_i , the LSTM Network will learn to forecast the value of the following time step \bar{X}_{i+1} . The

same process will be repeated where at the time step \bar{X}_{i+1} , the LSTM Network will learn to forecast the value of the following time step \bar{X}_{i+2} . The final forecast will be done at the time step \bar{X}_{N-1} where the LSTM network will learn to forecast the value at the final time step \bar{X}_N and therefore the training will be completed. The LSTM layer was specified to have 200 hidden units. The Adam optimization, a widely used extension of the stochastic gradient descent optimization was utilized for training the LSTM regression network. The LSTM regression network is used due to its high computational efficiency, smaller memory requirements and feasibility for large scale time series forecasting applications. The training was fixed at 250 epochs. The gradient threshold was set to 1 to prevent the gradients from exploding. The initial learning rate was specified to be 0.005 and this learning rate is dropped after 125 epochs by multiplication by a factor of 0.2. The Matlab Deep Learning toolbox is equipped with the 'PredictAndUpdateState' function to execute this step-by-step prediction when used together with a 'for' loop.

4. RESULTS

The LSTM networks were then used to forecast Solar Irradiance, Flux Calorimeter (Heat Meter 1 & 2) readings, solar collector inlet, and outlet temperatures. The LSTM forecasting was implemented on a HP 15-bw075AX laptop model with an AMD A12-9720P Radeon R7 processor and 4GB of RAM. The Root Mean Square Error (RMSE) values between the true and predicted values were calculated using Eq. (4) and tabulated in Table 4. The actual and forecast values of Solar Irradiance, Flux Calorimeter (Heat Meter 1 & 2) readings, solar collector inlet and outlet temperatures using test data are shown in Fig. 4, 5, 6, 7, and 8. Solar Irradiance, Collector Inlet and Outlet temperature could be forecast well with a low value of RMSE, which is less than 1. Flux Calorimeter readings could be forecast as well by using an LSTM Network. However, the RMSE values obtained were significantly higher since Flux Calorimeter readings could only be captured hourly. In contrast, Solar Irradiance, Collector Inlet and Outlet temperature are captured every 15 minutes resulting in more training data to be available for the LSTM Network. This result confirms that one of the constraints of forecasting is the sampling rate used by the sensors. If increased accuracy of the forecasting is desired, the sampling rate of the sensors should be increased. For comparison, these simulations were repeated using equivalent Gated Recurrent Units (GRU) instead of LSTM. It was found that lower RMSE values can be achieved using LSTM compared to GRU.

$$RMSE = \sqrt{\frac{\sum_{i=1}^N (\text{predicted} - \text{actual})^2}{N}} \quad (4)$$

In Fig. 4, the solar irradiance predicted values almost overlap the observed values, resulting in a lower RMSE value (0.43457). The lowest errors were for the samples that were within 1800 to 3000. The largest errors were for the samples with the range 600 to 1700. The largest errors were attributed to the fluctuation in solar irradiance which occurred between samples 600 to 1700 as shown in Fig. 4. The lower errors for samples in the range 1800 to 3000 were attributed to the steady decline in solar irradiance at this period as shown in Fig. 4.

In Fig. 5, the predicted collector outlet temperature values almost overlap the observed values, resulting in a lower RMSE value (0.80517). The error is relatively low throughout the samples except for the presence of an outlier at sample 1050. At this point,

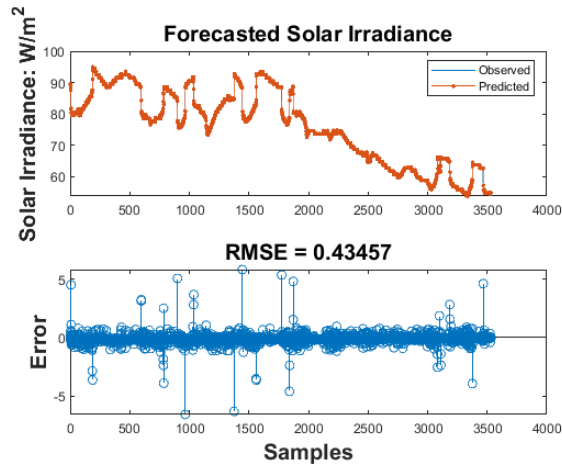


Fig. 4: Actual and Forecast Values of Solar Irradiance with Root Mean Square Error.

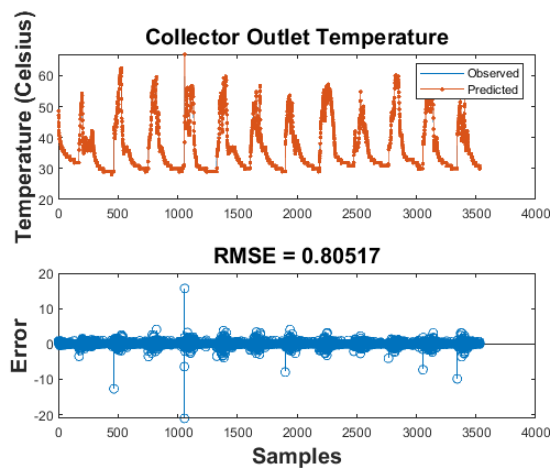


Fig. 5: Actual and Forecast Values of Collector Outlet Temperature with Root Mean Square Error.

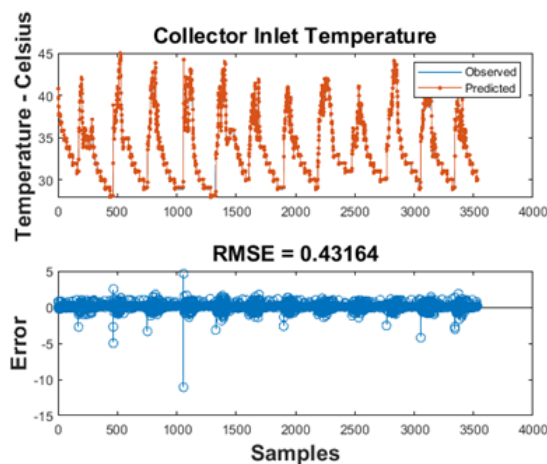


Fig. 6: Actual and Forecast Values of Collector Inlet Temperature with Root Mean Square Error.

there was a sudden rise in the collector outlet temperature and the LSTM model was not able to forecast this sudden rise in the collector outlet temperature accurately as compared to the rest of the samples in this time series data. Similarly in Fig. 6, the predicted collector inlet temperature also overlaps the observed value curves, resulting in a lower

RMSE value (0.43164). Although the overall error is relatively low, there is an outlier that also occurs at sample 1050 such that the LSTM model could not forecast the sudden rise in collector inlet temperature. The sudden change in the collector inlet and outlet temperature was due to the tripping of pumps that regulate the fluid circulation.

The RMSE values for forecasting Heat Meter 1 and 2 were recorded as 61.5091 & 23.8541 respectively and found to be higher than other parameters (solar irradiance, outlet & inlet temperatures). The main reason is that these energy meter readings are being logged hourly, therefore fewer samples of data are available for training the LSTM model resulting in a higher RMSE value. It can be observed from Fig. 7 that the error is higher for samples in the range from 20-70 but lower in other ranges. In the range from 20-70 the LSTM model had both underestimated and overestimated the readings for Heat Meter 1. The higher error at this range is attributed to the fluctuations in the Heat Meter 1 as well as the limitation in the number of samples of data available. Fig.8 shows the actual and forecast values for Heat Meter 2. A lower RMSE value was obtained for the forecasting of Heat Meter 2 values compared to Heat Meter 1. This lower RMSE value was due to less fluctuations occurring since the Heat Meter 2 readings steadily rise and decline in a predictable cyclic manner. Heat Meter 2 readings represent the final delivery of the water to the hot water tank and, therefore less fluctuations.

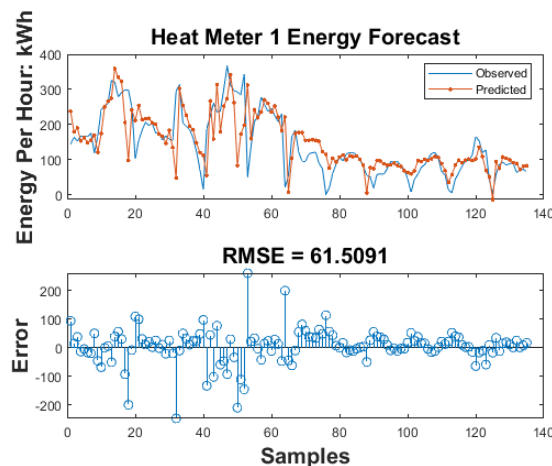


Fig. 7: Actual and Forecast Values of the First Flux Calorimeter Readings (Heat Meter 1) with Root Mean Square Error.

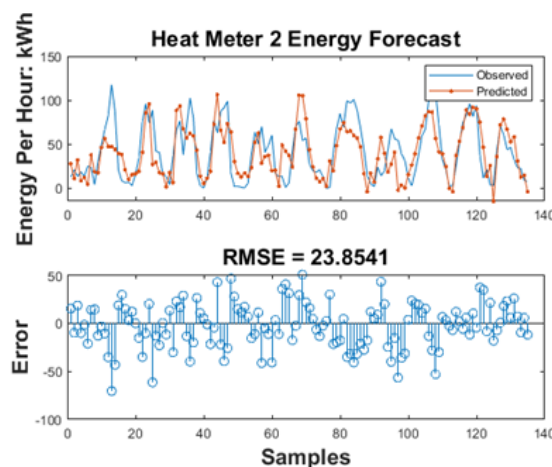


Fig. 8: Actual and Forecast Values of the Second Flux Calorimeter Readings (Heat Meter 2) with Root Mean Square Error.

The results presented in Fig. 4, 5, 6, 7, and 8 are summarized in Table 4. Overall results prove that LSTM is a suitable forecasting method to be applied at the backend of data logging systems for displaying forecast values and preliminary analysis. In particular, the forecast for Heat Meter 2 is beneficial for capacity planning of the factory to plan and meet the day ahead energy demand for their day-to-day operations.

Table 4: Total Number of Data Samples, Training Time and RMSE of LSTM Network Implementation

Parameter (s)	Total Data Samples	Training Time (Minutes)	RMSE (LSTM)	RMSE (GRU)
Solar Irradiance (W/m ²)	35337	410	0.43	0.85
Heat Meter 1 (kWh)	1354	30	61.51	72.34
Heat Meter 2 (kWh)	1354	28	23.85	35.76
Inlet Temperature (Celsius)	35340	430	0.43	0.78
Outlet Temperature (Celsius)	35340	415	0.80	1.53

5. CONCLUSION

In this study, a Solar Heat for Industrial Process (SHIP) system was designed and commissioned for implementation at a Malaysian Oleochemical factory. Five process parameters were recorded throughout a 4-month period namely Solar Irradiance, Solar Collector Inlet/ Outlet Temperature and flux calorimeter readings. In order to incorporate predictive maintenance, condition monitoring, assisting with planning, and commissioning existing renewable and non-renewable resources, two methods were used to forecast future values of these parameters namely LSTM and GRU. It was found that RMSE values obtained by applying LSTM were lower when compared to using Gated Recurrent Units (GRU). The results of this study reveal that LSTM can be integrated into the backend of existing data logging systems used in process industries in order develop websites that display forecasts of both engineering related parameters and also Return of Investments (ROI).

ACKNOWLEDGEMENT

The authors would like to thank the Malaysian Ministry of Higher Education for the funding received for this project under the Fundamental Research Grant Scheme - Grant No: FRGS19-057-0665. Furthermore, the authors would like to thank the IOT SATA Sdn. Bhd, the participating factory, and all supporting agencies for providing the technical data and support to carry out this research.

SUPPLEMENTARY MATERIALS

The codes for performing the forecasting and also the datasets used in this study are publicly available at the following Github repository:
<https://github.com/ahmadjazlan/LSTM-Solar-Parameter-Forecasting>

REFERENCES

- [1] Apergis N, Payne JE. (2012) Renewable and non-renewable energy consumption-growth nexus: Evidence from a panel error correction model, *Energy Economics*, 34(3): 733-738.

- [2] Can Tansel Tugcu, Ilhan Ozturk and Alper Aslan. (2012) Renewable and non-renewable energy consumption and economic growth relationship revisited: Evidence from G7 countries, *Energy Economics*, 34(6): 1942-1950.
- [3] Guney T. (2019) Renewable energy, non-renewable energy and sustainable development, *International Journal of Sustainable Development & World Ecology*, 26(5): 389-397.
- [4] Kim D, Kim KT., Park YK. (2020) A Comparative Study on the Reduction Effect in Greenhouse Gas Emissions between the Combined Heat and Power Plant and Boiler. *Sustainability*, 12(12): 5144-5155.
- [5] Yaguo L, Naipeng L, Liang, Ningbo L, Tao Y and Jing L. (2018) Machinery health prognostics: A systematic review from data acquisition to RUL prediction, *Mechanical Systems and Signal Processing*. 104: 799-834.
- [6] Zhang Y, Xiong R, He H, and Pecht MG. (2018) Long Short-Term Memory Recurrent Neural Network for Remaining Useful Life Prediction of Lithium-Ion Batteries. *IEEE Transactions on Vehicular Technology*, 67(7): 5695-5705.
- [7] Zhao R, Ruqiang Y, Jinjiang W, and Kezhi M. (2017) Learning to monitor machine health with convolutional Bi-directional LSTM networks, *Sensors*, 17(2): 273-290
- [8] Haedong J, Seungtae P, Sunhee W and Seungchul L. (2016). Rotating Machinery Diagnostics Using Deep Learning on Orbit Plot Images, *Procedia Manufacturing*, 5: 1107-1118.
- [9] Wu Y. et al. (2016) Google's neural machine translation system: bridging the gap between human and machine translation. Preprint at <https://arxiv.org/abs/1609.08144>.
- [10] Park K, Kim J and Lee J. (2019) Visual Field Prediction using Recurrent Neural Network. *Sci Rep* 9: 8385-8397.
- [11] Yuan L. (2017). Recurrent neural networks for classifying relations in clinical notes, *Journal of Biomedical Informatics*, 72: 85-95.
- [12] Lyu C, Chen B, Ren Y and Ji D. (2017) Long short-term memory RNN for biomedical named entity recognition. *BMC bioinformatics*, 18(1): 462-473.
- [13] Zhang F, Hu C, Yin Q, Li W, Li H-C and Hong W. (2017) Multi-Aspect-Aware Bidirectional LSTM Networks for Synthetic Aperture Radar Target Recognition. *IEEE Access*, 5: 26880-26891.
- [14] Chen C and Dai J. (2021) Mitigating backdoor attacks in LSTM-based text classification systems by Backdoor Keyword Identification. *Neurocomputing*, 452: 253-262.
- [15] Ogawa T, Sasaka Y, Maeda K and Haseyama M. (2018). Favorite Video Classification Based on Multimodal Bidirectional LSTM, *IEEE Access*, 6: 61401-61409.
- [16] Lan H, Gou Z and Cheng B. (2020) Regional difference of residential solar panel diffusion in Queensland, Australia, *Energy Sources, Part B: Economics, Planning, and Policy*, 15(1): 13-25.
- [17] Tsuchiya Y, Swai TA, Goto F. (2020) Energy payback time analysis and return on investment of off-grid photovoltaic systems in rural areas of Tanzania, *Sustainable Energy Technologies and Assessments*, 42(2020):100887-100894.
- [18] Ozcan O, Ersoz F. (2019) Project and cost-based evaluation of solar energy performance in three different geographical regions of Turkey: Investment analysis application, *Engineering Science and Technology, an International Journal*, 22(4): 1098-1106.
- [19] Gupta AK, Maity T, Anandakumar H, Chauhan YK. (2021) An electromagnetic strategy to improve the performance of PV panel under partial shading, *Computers & Electrical Engineering*, 90: 106896-106908.
- [20] Mert BD, Ekinci F and Demirdelen T. (2019) Effect of partial shading conditions on off-grid solar PV/Hydrogen production in high solar energy index regions, *International Journal of Hydrogen Energy*, 44(51): 27713-27725.
- [21] Niazi K, Khan HA, and Amir F. (2018) Hot-spot reduction and shade loss minimization in crystalline-silicon solar panels. *Journal of Renewable and Sustainable Energy* 10(3):033506-1 - 033506-8
- [22] Torres JPN, Nashih SK, Fernandes CAF and Leite JC. (2018) The effect of shading on photovoltaic solar panels. *Energy Systems* 9: 195-208.

- [23] Wang D, Qi T, Liu Y, Wang Y, Fan J, Wang Y and Du H. (2020) A method for evaluating both shading and power generation effects of rooftop solar PV panels for different climate zones of China, *Solar Energy*, 205: 432-445.
- [24] Akhter MN, Mekhilef S, Mokhlis H and Shah NM. Review on forecasting of photovoltaic power generation based on machine learning and metaheuristic techniques, *IET Renewable Power Generation* 13(7): 1009-1023
- [25] Akhter MN, Mekhilef S, Mokhlis H, Olatomiwa L and Muhammad MA. (2020) Performance assessment of three grid-connected photovoltaic systems with combined capacity of 6.575 kWp in Malaysia. *Journal of Cleaner Production*, 277: 123242.
- [26] Akhter MN, Mekhilef S, Mokhlis H, Ali R , Usama M , Muhammad MA. (2022) A hybrid deep learning method for an hour ahead power output forecasting of three different photovoltaic systems, *Applied Energy*, 307: 118185

APPENDIX

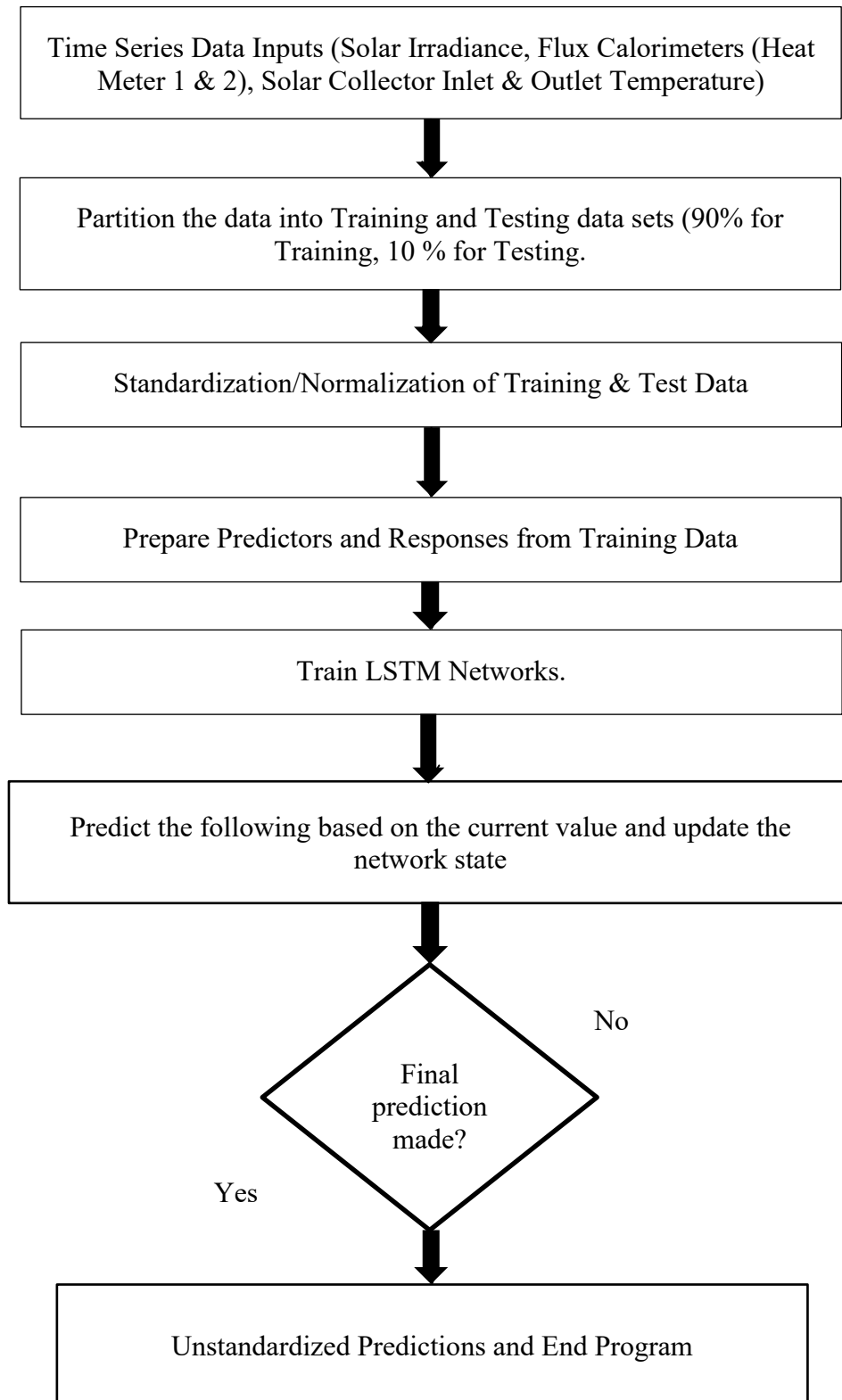


Fig. 9: Flowchart for MATLAB Programming.